Preprints of the 2012 20th Mediterranean Conference on Control & Automation (MED), Barcelona, Spain, July 3-6, 2012

Antiwindup Speed Technique for Sensorless Control of Synchronous Machine Using Saturation Feedback

Vasilios C. Ilioudis, *Student Member, IEEE,* and Nikolaos I. Margaris, *Member, IEEE*

***Abstract*—This paper presents a new antiwindup (AW) speed controller for salient-pole Synchronous Machine (SM) with rotor field winding. The control method is based on antwindup methodology using a sliding mode observer for controller gain adaptation. All the system variables are expressed in a γδ estimated rotating reference frame. Firstly, the unwanted windup phenomena due to the physical limitations are eliminated choosing suitably the controller transfer function. Secondly the speed converges asymptotically leading the saturation element very fast towards to the linear area of the actuator using a relatively simple AW control method. Simulation results demonstrate the effectiveness of the proposed antiwindup speed control method using Matlab/Simulink facility.**

Keywords-Synchronous Machine (SM); Antiwindup Controller (AWC); Modified back-EMF; Modified SM Model.

NOTATION

u_d, u_q = d-q axis voltages
i_d, i_q = d-q axis currents
r_s = stator resistance
L_d, L_q = d-q axis inductances
L_{md} = d-axis magnetizing inductance
λ_d, λ_q = d-q axis magnetic fluxes
u_γ, u_δ = γ-δ axis voltages
i_γ, i_δ = γ-δ axis currents
i_{df} = rotor field exitation current
λ_γ ,λ_δ = γ-δ axis magnetic fluxes
$\lambda_{m\gamma}$, $\lambda_{m\delta}$ = γ-δ axis partial magnetic fluxes
E_γ, E_δ = γ-δ axis modified back EMF
p = number of pole pairs
θ = angular position
T_e = electrical motor torque
T_l = load torque
J = inertia of the rotor
B = rotor damping
ω = angular speed

I. INTRODUCTION

SYNCHRONOUS motors (SM) and especially Permanent Magnet Synchronous Machine (PMSM) are widely used in many industrial applications that require high reliability and efficiency. Effective control schemes of a SM such as field oriented and direct torque require accurate and robust controllers for adjustable speed drive applications such as hybrid vehicles, robots and machine tools. Normally, for applications of variable speed motor drives, the power to AC motors is provided via Voltage Source Inverters (VSI) using a Space Vector Pulse Width Modulation (SVPWM) method.

In most applications the overall control system includes two inner PI controllers for the stator currents and one outer PI controller for the rotor speed supposing that they operate linearly. Since excessive large control actions could destabilize or in the worst case damage the system, the control outputs are limited to their maximum / minimum values. Because of the physical limitations of the inverter-motor system, the q-axis current generated by the PI speed controller is practically limited to prescribed values (maximum / minimum current) depended on the magnetic saturation, the inverter maximum current limit and the overheating of stator windings. These limits have severe consequences for AC motor speed control introducing the drive system into an unstable mode when the PI speed controller saturates. In this case of saturation the output is uncontrolled since it could not be affected by its input anymore. Especially, the integral action of the PI speed controller accumulates the errors causing a large overshoot and slow settling time on the speed response. This is the so-called windup phenomenon. For high performance speed control of synchronous machine, an antiwindup speed controller with tracking gain is used to cancel any problem due to current limiters.

To overcome the classical problem of integrator windup due to saturation (so-called windup phenomenon) several approaches have been developed [3], [5]-[9]. These antiwindup (AW) techniques are mainly classified into two strategies, the methods that depended and ones that do not depended on saturation. Integrator windup could be avoided by setting the integral part to proper value when the PI controller saturates. The control method called AW PI with dead zone uses a dead zone element to control the limit of integral part of the PI controller, while the AW PI conditioned method is based on canceling the integral action when the saturation appears [8]. Also the AW PI tracking method uses the difference in the saturation part of the controller multiplied by a gain to reduce the integrator

Manuscript received January 18, 2012.

V. C. Ilioudis is currently PhD student in the Department of Electrical and Computer Engineering at Aristotle University of Thessaloniki, Thessaloniki, GR 541 24, Greece (phone: +302392025893; fax: +302310791256; e-mail: ilioudis@teithe.gr).

N. I. Margaris is with the Electrical and Computer Engineering Department, Aristotle University of Thessaloniki, Thessaloniki, GR 541 24 Greece (e-mail: margaris@eng.auth.gr).

978-1-4673-2529-5/12/$31.00 ©2012 IEEE

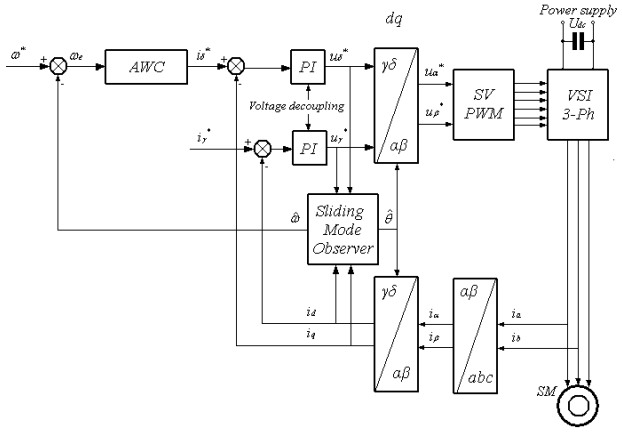

Figure 1. The speed control system of SM with SMO.

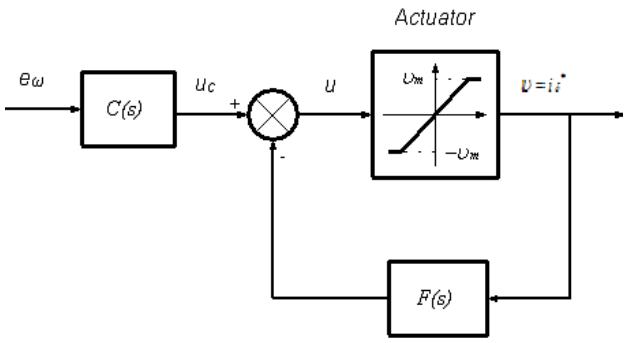

Figure 2. Antiwindup Speed Controller of Synchronous Machine with a Series Form.

action [13]. An improvement of the later method is the AW PI with tracking gain method, which uses an adjustment of the feed back gain to control the overshoot response.

The speed control method presented in this paper is implemented using a simple antiwindup controller with proper choice of its transfer functions. To avoid the windup phenomenon, a finite-time convergent controller based on the saturation block output regulates the speed controller performance. Once the saturation element operates in the linear area the error between the speed reference and the estimated speed, witch is obtained by means of a modified back EMF observer, is getting very close to 0. Fig. 1 shows in block diagram a SM sensorless speed control system based on an AWC with series form. The robustness of the proposed speed control algorithm is validated by simulation experiments performed on a salient-pole SM fed by VSI with SVPWM at 5-8kHz switching frequency.

II. Modified Model of SM and Sliding Mode Observer

A. Modified Model of SM in γ-δ Reference Frame

The proposed AWC is applied on a SM mathematical model defined in an estimated γ-δ reference frame, which is rotating at an angular velocity $\hat{\omega}$ and lagging behind the d-q reference frame by electrical angle $\bar{\theta}$ ($\bar{\theta}=\theta-\hat{\theta}$) [18]. Considering $\dot{\bar{\theta}}=\bar{\omega}$, the γ-δ axis SM model is given as follows

$$L_q\begin{bmatrix}\dot{i}_\gamma\\ \dot{i}_\gamma\end{bmatrix}=-r_s\begin{bmatrix}i_\gamma\\ i_\delta\end{bmatrix}-\hat{\omega}L_qJ_m\begin{bmatrix}i_\gamma\\ i_\delta\end{bmatrix}+\begin{bmatrix}u_\gamma\\ u_\delta\end{bmatrix}+\begin{bmatrix}E_\gamma\\ E_\delta\end{bmatrix}-\begin{bmatrix}\varphi_\gamma\\ \varphi_\delta\end{bmatrix} \quad (1)$$

The terms E_γ and E_δ represent the modified back EMF in γ-δ axis given by

$$\begin{bmatrix}E_\gamma\\ E_\delta\end{bmatrix}=-\omega J_m\lambda_{mdL}\begin{bmatrix}\cos\bar{\theta}\\ \sin\bar{\theta}\end{bmatrix}$$

and $\varphi_{\gamma\delta}$ is defined as

$$\varphi_{\gamma\delta}=\begin{bmatrix}\varphi_\gamma\\ \varphi_\delta\end{bmatrix}=\begin{bmatrix}\dot{\lambda}_{mdL}\cos\bar{\theta}\\ \dot{\lambda}_{mdL}\sin\bar{\theta}\end{bmatrix}$$

Here λ_{mdL}, J_m are respectively the modified magnetic flux and the skew symmetric matrix defined by

$$\lambda_{mdL}=\left[L_{md}i_{df}+\left(L_d-L_q\right)i_d\right]=\left[\lambda_{md}+\left(L_d-L_q\right)i_d\right]$$

$$J_m=\begin{bmatrix}0 & -1\\ 1 & 0\end{bmatrix}$$

B. Sliding Mode Observer (SMO) of SM

Rotor position and speed information is provided to AWC by means of a sliding mode observer. In sliding manifold design, stator current errors between their measured and estimated values are used as sliding surfaces, that is $s_\gamma=\bar{i}_\gamma=i_\gamma-\hat{i}_\gamma$ and $s_\delta=\bar{i}_\delta=i_\delta-\hat{i}_\delta$. The used stator flux/current observer is defined by

$$L_q\dot{\hat{i}}_\gamma=-\hat{r}_si_\gamma+u_\gamma+\hat{\omega}L_qi_\delta+K_\gamma\operatorname{sgn}\bar{i}_\gamma \quad (2a)$$

$$L_q\dot{\hat{i}}_\delta=-\hat{r}_si_\delta+u_\delta-\hat{\omega}L_qi_\gamma+\hat{E}_\delta+K_\delta\operatorname{sgn}\bar{i}_\delta \quad (2b)$$

Here K_γ, $K_\delta > 0$ are the observer gains. Also $\hat{r}_s$ and $\hat{E}_\delta$ are the estimated stator resistance and back EMF respectively.

After finite time t_n, the sliding surface is reached ($s=s_{\gamma\delta}=0$). Using the equivalent control method, then estimated back EMF, speed and position dynamics are respectively given by

$$\dot{\hat{E}}_\delta=c\dot{\bar{E}}_\delta \quad (3a)$$

$$\dot{\hat{\omega}}=-\gamma_\omega\hat{E}_\delta E_\gamma \quad (3b)$$

$$\dot{\hat{\theta}}=\hat{\omega} \quad (3c)$$

Here c, $\gamma_\omega > 0$ are the back EMF observer gains.

III. Antiwindup Controller Analysis of SM

A. Speed/Torque Controller of SM with Current Limiter

Normally, in control system of a SM, the dynamics of both current controllers is designed to be much faster than the ones of speed controller. Also, in the case of speed

control under the base speed, the i_γ^* current is usually set to zero ($i_\gamma^*=0$) and therefore the torque command T_e^* expressed by the i_δ^* current is proportional of the speed controller output.

If a fast current control scheme is employed, the current dynamics can be neglected and the variable speed motor drive can be considered as a first order system give by

$$\dot{\omega} = -\frac{B}{J}\omega + \frac{(T_e - T_l)}{J} \tag{4}$$

Considering that the factor due to rotor viscous is very small, (4) could be simplified as follows

$$\dot{\omega} = \frac{(T_e - T_l)}{J} = \frac{3p\lambda_{md}}{2J} i_\delta = k_t i_\delta \tag{5}$$

Here k_t is the torque constant.

In practical applications of SM speed control there is a saturating element between the speed controller and the δ-axis current controller. It is assumed that the nonlinearity of the saturation type element of the stator current limiter is expressed by

$$\upsilon = \begin{cases} u & if \quad |u| \le \upsilon_m \\ \upsilon_m \operatorname{sgn} u & if \quad |u| > \upsilon_m \end{cases} \tag{6}$$

Here the variable u represents the input to the δ-axis current limiter and υ_m is the maximum stator current allowed. Therefore the variable υ represents the input to inner δ-axis current controller, which is the δ-axis reference current i_δ^*. In the no ideal situation the control action is limited regardless of the control system's output u (see Fig. 2).

B. Analysis of Antiwindup Controller (AWC)

For high performance speed control of synchronous machine, an antiwindup speed controller (AWSC) with series form is used. Fig. 2 shows a block diagram of the AWC for the controlled SM.

An essential feature of this antiwindup technique is the choice of the transfer functions *C(s)* and *F(s)* according to the desired dynamical specifications of the closed-loop system. To implement the AWC analysis, the controller is considered in the sense of Laplace function [5]. The output u_c is expressed in the following form

$$U_c(s) = C(s)E_\omega(s) \tag{7}$$

Let the transfer function *C(s)* be *C(s)=P(s)/R(s).* So (7) can be re-written more analytically as follows:

$$U_c(s) = \frac{P(s)}{R(s)} E_\omega(s) \tag{8}$$

The AW controller can be implemented by means of saturation feedback, as it is shown in Fig. 2. Assuming that the transfer function of saturation feedback *F(s)* is defined by

$$F(s) = \frac{Q(s) - R(s)}{R(s)} \tag{9}$$

Where $P(s) = p_n s^n + p_{n-1}s^{n-1} + \ldots + p_0$ is a polynomial in complex plane with the Laplace variable *s*. In addition the polynomials $R(s) = s^n + r_{n-1}s^{n-1} + \ldots + r_0$ and $Q(s) = s^n + q_{n-1}s^{n-1} + \ldots + q_0$ are monic. Choosing properly the above transfer functions assures the asymptotic stability of the controlled system for both operating modes of the current limiter, linear ($\upsilon=u$) and saturation ($\upsilon \neq u$) [1], [3].

Setting the current limiter error $\Delta u=u-\upsilon$ and considering Fig. 2, the Laplace transform of the control input of the actuator is given by

$$U(s) = \frac{P(s)}{R(s)} E_\omega(s) - \left[\frac{Q(s) - R(s)}{R(s)}\right]\left[U(s) - \Delta U(s)\right]$$

or

$$\left[1 + \frac{Q(s) - R(s)}{R(s)}\right] U(s) = \frac{P(s)}{R(s)} E_\omega(s) + \left[\frac{Q(s) - R(s)}{R(s)}\right] \Delta U(s) \tag{10}$$

After some calculations the last relation could be rewritten in a simplified form as follows

$$U(s) = \frac{P(s)}{Q(s)} E_\omega(s) + \left[\frac{Q(s) - R(s)}{Q(s)}\right] \Delta U(s) \tag{11}$$

or

$$U(s) = U_E(s) + U_\Delta(s) \tag{12}$$

Here

$$U_E(s) = \frac{P(s)}{Q(s)} E_\omega(s) = C_E(s) E_\omega(s) \tag{13}$$

and

$$U_\Delta(s) = \frac{Q(s) - R(s)}{Q(s)} \Delta U(s) = C_{\Delta u}(s) \Delta U(s) \tag{14}$$

Here $C_E(s)=P(s)/Q(s)$ and $C_{\Delta u}(s)=[Q(s)-R(s)]/Q(s)$.

Equation (12) implies that the control input u ($u=i_\delta^*$) inner *δ-axis* current controller could be written as a sum of the auxiliary control inputs u_E and u_Δ defined by (13) and (14) respectively (see Fig. 1 and Fig. 2). Essentially the antiwindup compensation problem is divided into two separated tasks making it easier to reach speed controller stability. Here the antiwindup controller is considered as closed loop system implementing an inner fast loop for the current limiter error Δu. Control action in (14) is to reduce saturation effect ($\Delta u \to 0$) and converge very fast causing the speed controller to operate into linear area. Using (13), (14) and (12) it results that

$$\lim_{\Delta u \to 0} U(s) = U_E(s) = \frac{P(s)}{Q(s)} E_\omega(s) \tag{15}$$

In the case of $\Delta u=u-\upsilon=0$, speed controller operates linearly depending only on transfer function $C_E(s)=P(s)/Q(s)$.

An exponential stability occurs when all the poles of *Q(s)*

polynomial are in left half of the complex plane. The transfer functions *Q(s)* and *R(s)* are chosen to achieve the desired stability properties of the AW controller such that to lead both speed and current limiter errors to zero.

IV. Simulation Results

To evaluate the proposed AWC, a controller-observer scheme has been tested on a salient-pole SM with rotor field winding at a wide speed rage from 600rpm up to 3000rpm. The parameters of the tested SM and are listed in Table I. In the implemented sensorless control, rotor speed and position information are provided to AWC through a sliding mode observer (SMO) [18]. The parameters of the SMO, speed and modified back EMF observer are listed in Table II. Also the chosen polynomials *P(s)*, *Q(s)* and *R(s)*, are of first order and listed in Table III. Their coefficients are depended on the operating conditions, SM parameters and sliding mode observer (SMO) gains. Proper choice of *P(s)*, *Q(s)* and *R(s)* polynomials forces the controller to operate linearly and therefore cancels any problem due to current limiter saturation. All the experiments on the developed antiwindup algorithm are carried out using the Matlab/Simulink facility. The inverter switching frequency is 5-8kHz with 520V dc voltage of power supply while the rotor winding magnetizing current i_{df} is equal to 1.5 A and rotor dumping *B* is supposed to be almost zero.

Fig. 3 shows the system response with AWC at nominal speed (3000rpm). The applied antiwindup compensation scheme results to a lower overshoot compared to a conventional PI controller achieving significant closed-loop performance. Fig. 4 shows the γ- and δ-axis stator currents provided by the antiwindup algorithm. Fig. 5 shows the 3-phase stator currents focused at the point neighborhood, where the rotor speed is reversing. The speed tracking is shown in Fig. 6 under antiwindup controller correcting the actuator saturation effects.

Simulation results (Fig. 3 through Fig. 6) are considered system response at high-speed range with 4.7A inverter current limit and stepwise changes of speed. Although the speed command is reversed from 50*2π rad/s (3000rpm) to –50*2π rad/s (-3000rpm) at time t_0 = 5s the estimated speed follows exactly the change of the actual speed regardless the cross zero point of the modified back-EMF [20]. Fig. 7 shows the system response using AWC at medium frequency rage speed (1500rpm) with an external load application of 2N.

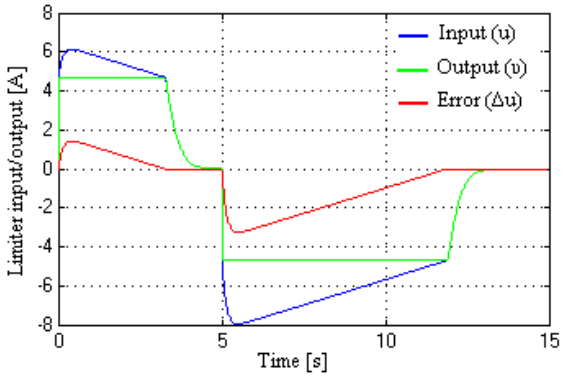

Figure 3. Antiwindup controller (AWC) response for step change of speed 0-50*2π rad/s (3000 rpm) with no load. At time t_0=5s the speed was reversed.

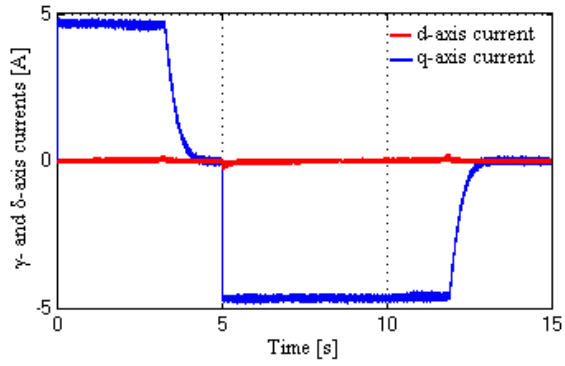

Figure 4. Responses of d- and q-axis stator currents for step change of speed 0-50*2π rad/s (3000 rpm) with no load. At time t_0=5s the speed was reversed.

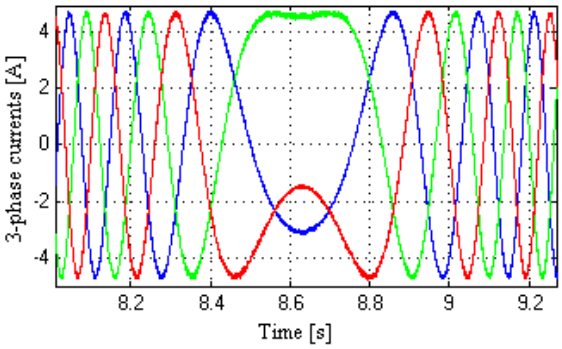

Figure 5. A detailed description of 3-phase stator currents (a, b and c) response for step change of speed 0-50*2π rad/s (3000 rpm) with no load. At time t_0=5s the speed was reversed.

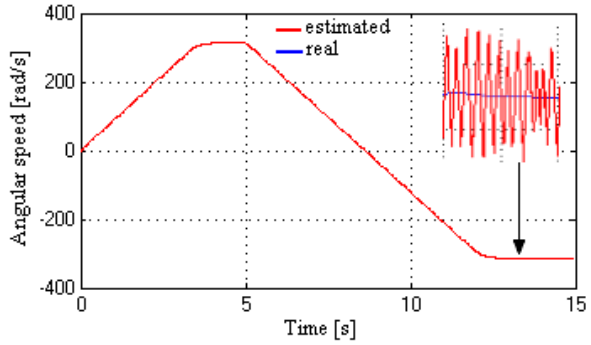

Figure 6. Rotor speed response for step change of speed 0-50*2π rad/s (3000 rpm) with no load. At time t_0=5s the speed was reversed.

Performance optimization under saturation constraints is achieved by means of the antiwindup controller even at the presence of external torque disturbances. Fig. 8 shows the γ- and δ-axis stator currents provided by the antiwindup algorithm and how the torque load of 2N affects these. The three phase currents of the stator are shown in Fig. 9, where the speed reversing point is shown in more details. Also simulation results (Fig. 7 through Fig. 9) present system response at medium-speed range under torque load with 8.0A inverter current limit and stepwise changes of speed. As previously, the speed command is reversed from 25*2π rad/s (1500rpm) to –25*2π rad/s (-1500rpm) at time t_0 = 4s as well.

Fig. 10 shows the antiwindup controller performance at low frequency rage (600rpm or 10Hz) without external load application. Fig. 11 shows the response of motor produced torque, while Fig. 12 shows the rotor speed tracking.

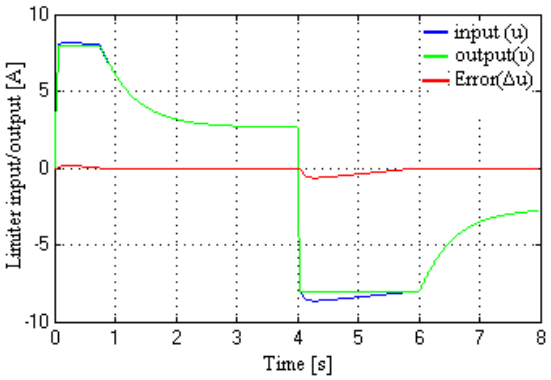

Figure 7. Antiwindup controller (AWC) response for step change of speed 0-25*2π rad/s (1500 rpm) with a load of 2 N. At time t_0=4s the

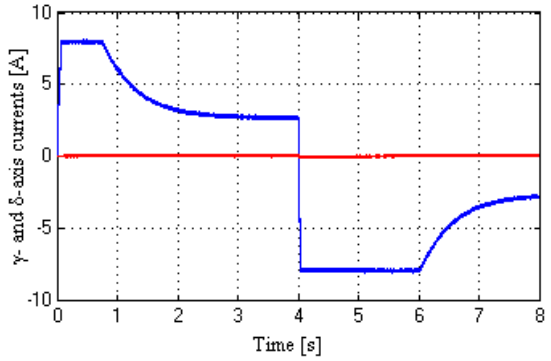

Figure 8. Responses of d- and q-axis stator currents for step change of speed 0-25*2π rad/s (1500 rpm) with load of 2N. At time t_0=4s the speed and torque ware reversed.

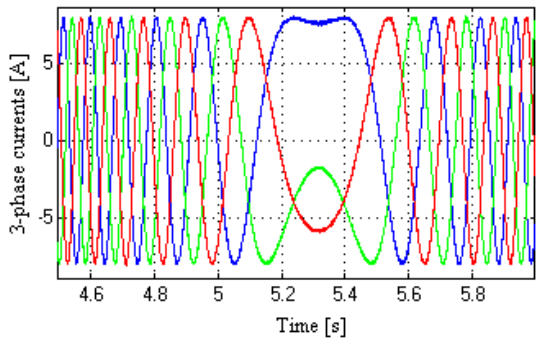

Figure 9. A detailed description of 3-phase stator currents (a, b and c) response for step change of speed 0-25*2π rad/s (1500 rpm) with load of 2N. At time t_0=4s the speed and torque ware reversed.

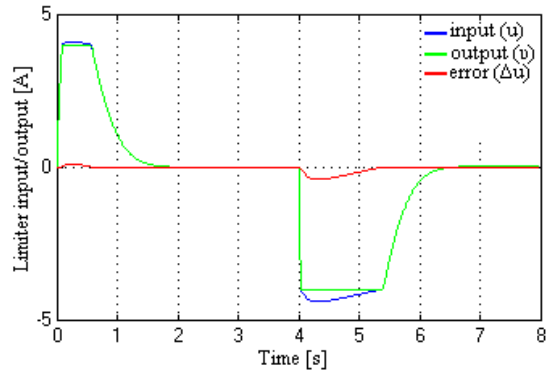

Figure 10. Antiwindup controller (AWC) response for step change of speed 0-10*2π rad/s (600rpm) with no load. At time t_0=4s the speed was reversed.

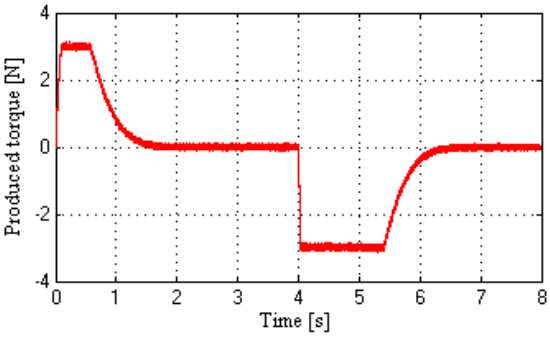

Figure 11. Motor torque response for stepwise change of speed 0-10*2π rad/s (600 rpm) with no load. At time t_0=4s the speed was reversed.

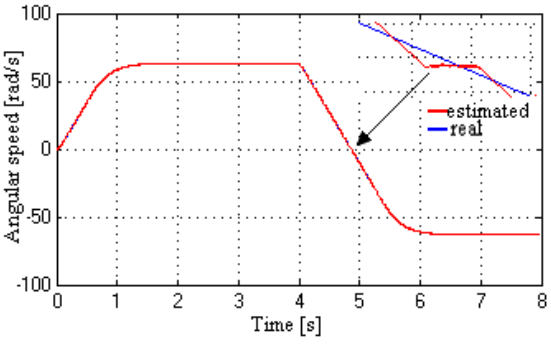

Figure 12. Rotor speed response for step change of speed 0-10*2π rad/s (600 rpm) with no load. At time t_0=4s the speed was reversed.

TABLE I
PARAMETERS OF SYNCHRONOUS MACHINE WITH ROTOR FIELD WINDING

Symbol	Quantity	Expressed in SI
S	electric power	5.5 kVA
$cos\varphi$	electric power coefficient	0.8
$V_{l\text{-}l}$	line to line voltage	380 V
r_s	stator resistance	2.5 Ω
L_{md}	d-axis magnetizing inductance	0.360 H
L_d	d-axis inductance	0.400 H
L_q	q-axis inductance	0.210 H
J	moment of inertia	0.039 kgm^2
p	magnetic pole pairs	1
ω_m	mechanical angular speed	3000 rpm

TABLE II
PARAMETERS OF SLIDING MODE AND MODIFIED BACK EMF OBSERVERERS

Symbol	Quantity	Expressed in SI
K_γ	γ-axis gain of SMO	18000
K_δ	δ-axis gain of SMO	18000
γ_r	stator resistance gain	80
γ_ω	angular speed observer gain	350
c	modified back-EMF observer gain	80

TABLE III
POLYNOMIALS OF ANTIWINDUP CONTROLLER

Symbol	Polynomial
$P(s)$	1
$Q(s)$	$s+5$
$R(s)$	$s+8$

At low speed range, the inverter current limit is set 4.0A and the speed is changed stepwise at time t_0 = 4s from 10*2π to -10*2π. Simulation results in Fig. 3, Fig. 7 and Fig. 10 demonstrate the effectiveness of the antiwindup control algorithm achieving fast speed response and canceling the effects of actuator saturation.

Examining the waveforms of Fig. 3, Fig. 7 and Fig. 10 it can be seen that the dynamic speed control performance of the SM with AW controller is better than that with conventional PI controller, since the current overshoot is considerably decreased achieving better speed response. In addition exploring the waveforms of Fig. 6 and Fig. 12, it can be seen as well, that the entire system with AW controller has more robustness in a wide speed range.

V. CONCLUSION

The proposed technique introduces an improved SM rotor speed control algorithm implementing an antiwindup (AW) methodology. In fact, this controller is based on a back-calculation anti-windup technique using proper transfer functions. Any effect caused by the presence of saturation nonlinearity is effectively compensated very fast despite the existence of the applied external torque disturbances and motor parameter changes.

The developed speed AWC can achieve high-accuracy speed control, less overshoot, fast dynamic response at an extensive range of speed. The controller-observer system has been tested on a salient-pole SM at a wide speed rage from almost zero speed to above the base speed keeping good performance characteristics. In addition this work could be extended to apply to other type of SM motors as well including PMSM (IPM and SPM). Simulation results show its robustness and high performance.

REFERENCES

[1] P. C. Krause, O. Wasynczuk, and S. D. Sudhoff, "Analysis of electric machinery and drive systems", 2nd ed., *Wiley-IEEE*, New York, 2002.

[2] Antonio Visioli, "Practical PID Control (Advances in Industrial Control)", *Springer-Verlag London Limited*, 2006.

[3] Karl Johan Aström and Richard M. Murray, Feedback Systems – an introduction for scientists and engineers, 2008

[4] J-J. E. Slotine and W. Li "Applied Nonlinear Control", *Prentice-Hall International, Inc.*, 1991.

[5] V. M. Becerra, "Actuator saturation and anti-windup compensation", *Lectures on Nonlinear Control*, University of Reading, January 2009.

[6] Hwi-Beom Shin,"New Antiwindup PI Controller for Variable-Speed Motor Drives", *IEEE Trans. Ind. Electron.*, vol. 45, no. 3, pp. 445-450, June 1998.

[7] Phil March, and Matthew C. Turner, "Anti-Windup Compensator Designs for Nonsalient Permanent-Magnet Synchronous Motor Speed Regulators", *IEEE Trans. Industry Applications,*, vol 45, no. 5, pp. 1598-1609, Sept./Oct. 2009.

[8] A. Visioli, "Modified Anti-windup Scheme for PID Controllers", *IEE Proceedings of Control Theory and Applications*, vol. 150, no 1, pp. 49-54, January 2003.

[9] Jul-Ki Seok, "Frequency-Spectrum-Based Antiwindup Compensator for PI-Controlled Systems", *IEEE Trans. Ind. Electron.*, vol. 53, no. 6, pp. 1781-1790, Dec. 2006.

[10] Y. Peng, D. Vrancic, and R. Hanus, "Anti-windup, bumpless, and conditioned transfer techniques for PID controllers", *IEEE Control Systems Mag.*, vol. 16, no. 4, pp. 48–57, Aug. 1996.

[11] Gene Grimm, Jay Hatfield, Ian Postlethwaite, Andrew R. Teel, Matthew C. Turner, and Luca Zaccarian, "Antiwindup for Stable Linear Systems With Input Saturation: An LMI-Based Synthesis", *IEEE Trans. Automat. Control*, vol. 48, no. 9, pp. 1509-1524, Sept. 2003.

[12] A. S. Hodel and C. E. Hall, "Variable-structure pid control to prevent integrator windup", *IEEE Trans. Industrial Electronics*, vol. 48, no. 2, pp. 442-451, April 2001.

[13] C. Bohn and D. P. Atherton, "An Analysis Package Comparing PID Antiwindup Strategies", *IEEE Systems Magazine*, vol. 15, no. 2, pp. 34-40, April 1995.

[14] Jong-Woo Choi, and Sang-Cheol Lee, "Antiwindup Strategy for PI-Type Speed Controller", *IEEE Trans. Ind. Electronics*, vol. 56, no. 6, pp. 2039-2046, June 2009.

[15] R. Hanus, M. Kinnaert and J.-L. Henrotte, "Conditioning technique, a general anti-windup and bumpless transfer method", *Automatica*, vol.v23, no. 6, pp. 729-739, November 1987.

[16] Yu-Sheng Lu, "Non-overshooting PI control of variable-speed motor drives with sliding perturbation observers", *ELSEVIER, Mechatronics*. vol. 15, pp.1143-1158, March 2005.

[17] Kapila, V. and K. Grigoriadis, "Actuator saturation control", *Marcel Dekker Inc.*, New York, 2002.

[18] V. C. Ilioudis and N. I. Margaris, "Speed and position estimation technique for PMSM based on modified machine model", Proceedings of the *12th International Conference on Optimization of Electrical and Electronic Equipment (OPTIM 2010)*, Brasov, Romania, pp. 407 - 415, 20-22 May 2010.